PLATE ANCHOR GROUPS PULLED VERTICALLY IN SAND

By James D. Geddes,[1] Fellow, ASCE, and Edward J. Murray[2]

ABSTRACT: Results are presented of model-scale vertical pulling tests carried out on groups of square anchor plates in row and square configurations. The tests were carried out at a single depth of embedment, which ensured shallow anchor behavior in the sand placed at a constant dry density. It is shown that the load-displacement relationships for all groups may be reduced to a common curve. The load-carrying capacity of a group of anchor plates increases with the spacing between the individual plates up to a limiting critical value, and it is demonstrated how the results of pulling tests with different numbers of plates in a group may be described in a simple unifying manner. A possible means of predicting the effect of interaction on the uplift capacity of both model- and full-scale anchors in row configurations is suggested. For laboratory tests on a linear group of five anchors, it is shown that the end anchors attain the highest loads but all loads converge to an equal value as the spacing increases to the critical value.

INTRODUCTION

The behavior of groups of anchors is of considerable importance, yet relatively little has been published on the topic. The testing reported herein is aimed at developing an understanding of the interaction between anchors or footings subject to tensile loads. The tests may be taken as representing, at small scale, concrete slab anchors, grillage anchors, or other large plate-like anchorages. Such anchors have been used to resist wind loading and overturning of transmission towers or other guyed structures. However, anchors have been used for many other purposes, including resisting hydrostatic uplift of buried structures below the water table. Conversely, the testing may be taken as simulating the tension loads on pad footings where subsidence occurs, such as in areas of mining or filled ground.

Laboratory work on the horizontal translation of rows of three square plates in sand has been reported by Hueckel (1957), who found that, below a particular spacing of the plates, the ultimate load capacity of the group decreased as the spacing was further reduced. Smith (1962) also performed tests on the horizontal translation of groups of three anchors in sand, under full-scale field conditions, and reported results in broad agreement with the findings of Hueckel. A further study of the interference effects of horizontally translated anchors in sand is that of Neely (1971). Using square plates, he examined, at laboratory scale, the effect of horizontal spacing on rows of two and four plates at different depth/plate size ratios. The work was extended to cover the case of the horizontal translation of a pair of plates placed vertically one above the other with an overall height/plate size ratio of five.

Laboratory vertical pulling tests on groups of circular anchors in sand have been reported by Hanna et al. (1972). The anchors were in groups of up to 25, at various spacings and at depth/diameter ratios of six and 12. The ultimate group resistances were compared with the theoretical values of Meyerhof and Adams (1968), and it was concluded that, although the theory predicted behavioral trends, the theoretical failure values were considerably in error. Meyerhof (1973a,b) has also tentatively suggested theoretical approaches for the uplift of horizontal anchors under oblique loads and inclined anchorages.

Laboratory tests on steel ball anchors embedded in sand and pulled at angles of inclination up to 55° from the vertical have been reported by Larnach (1972, 1973) for two anchors and for line groups of three and five anchors. In these tests the depth/diameter ratio was constant at 16, thus ensuring deep anchor behavior. He reported that the initial slope of the load pullout curve for grouped anchor plates is essentially linear and independent of inclination, spacing, and number of anchors in the group. In the vertical uplift of a line of five anchors, the two outside anchors exhibited the highest pullout resistance, the central anchor of the group recorded the next highest resistance, while the lowest resistance was associated with the two remaining interior anchors.

The present paper describes the behavior, at laboratory scale, of groups of square steel plates when pulled vertically upward in a very dense sand (Murray 1977). One depth of embedment was used throughout. There is, therefore, no exact parallel between the results reported and the foregoing experimental investigations.

LABORATORY TESTS

The sand used in the tests had 95% of its particles within the size range of 0.15–0.50 mm, a uniformity coefficient of 1.62, and an effective grain size of 0.16 mm. The average unit weight of the sand, compacted by vibration in the test bin, was 16.5 kN/m^3, with a variation of density during the whole program of ±0.9%, as measured using small tins embedded within the sand during placement. The relative density was 85.9%.

At this density, shear box tests yielded peak shear strength parameters of $c' = 0$ and $\phi' = 43.6°$. Modified shear box tests gave an interface friction angle of 10.6° for the sand in contact with polished steel plates, of the kind used in the uplift tests.

Vertical uplift tests were carried out on the following anchor assemblies: a configuration of two square plates (with edges parallel) at different spacings; a line group of five square plates at similar spacings to the paired plates; and groups of four square plates placed in square configurations, again with similar spacings. To ensure that the anchor plates did not move during sand placement and compaction, the tie-rods from the anchor plates were clamped, and the plates rested on a template designed to restrict their movements except when subsequently subjected to uplift.

A displacement-controlled loading system was used in the uplift tests. It was thus possible to record in detail the postpeak behavior. The group load-displacement responses were obtained from proving ring and displacement dial gauge readings, while the loads on the individual anchor plates were continuously monitored using load cells attached to the tops of the individual tie-rods. The general test arrangement is shown in Fig. 1.

[1]Emeritus Professor, Consultant; formerly, Head of Div. of Civ. Engrg., School of Engrg., Univ. of Wales Coll. of Cardiff, Cardiff, CF2 1XH U.K.

[2]Dir., Murray Rix Geotechnical, 5A Regent Court, Hinckley, LE10 0AD, Leicestershire, U.K.

Note, Discussion open until December 1, 1996. To extend the closing date one month, a written request must be filed with the ASCE Manager of Journals. The manuscript for this paper was submitted for review and possible publication on May 2, 1994. This paper is part of the ***Journal of Geotechnical Engineering***, Vol. 122, No. 7, July, 1996. ©ASCE, ISSN 0733-9410/96/0007-0509–0516/$4.00 + $.50 per page. Paper No. 8369.

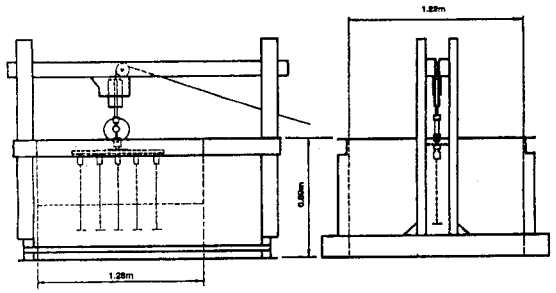

FIG. 1. Details of Anchor Test Rig

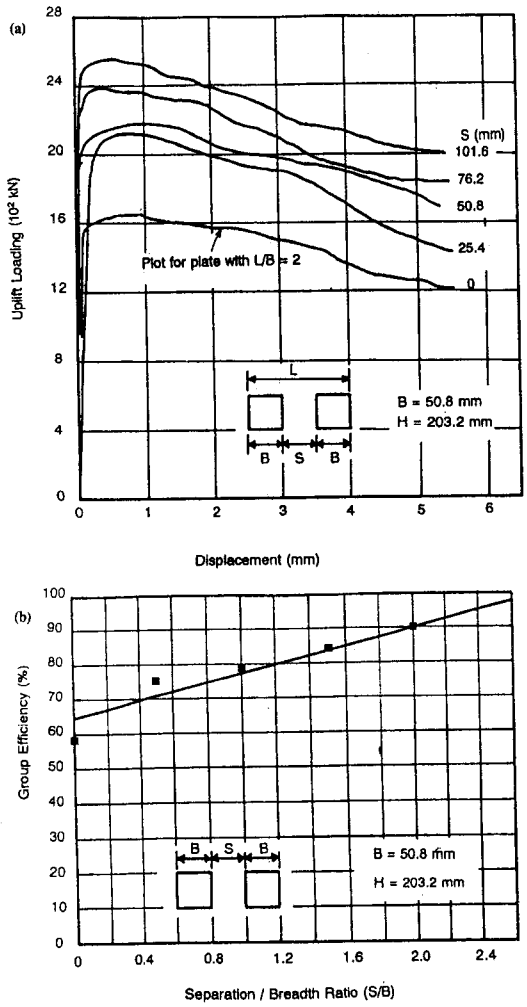

FIG. 2. Two Square Plate Configuration: (a) Load-Displacement Curves; (b) Group-Efficiency versus Separation/Breadth Ratio

The depth of embedment within the sand (H/B = 4 for all tests) was chosen to ensure that the rupture surfaces reached the sand surface, i.e., shallow behavior. The experimental results are initially presented as plots of uplift load against displacement, and as plots of group efficiency against separation ratio (S/B). The latter is defined as the gap between the edges of successive plates divided by plate size, and the former is defined in the manner adopted by Hanna et al. (1972) and Larnach (1972, 1973)

$$\text{group efficiency (\%)} = \frac{\text{peak load of group of } N \text{ plates} \times 100}{N \times \text{peak load of a single isolated plate}} \quad (1)$$

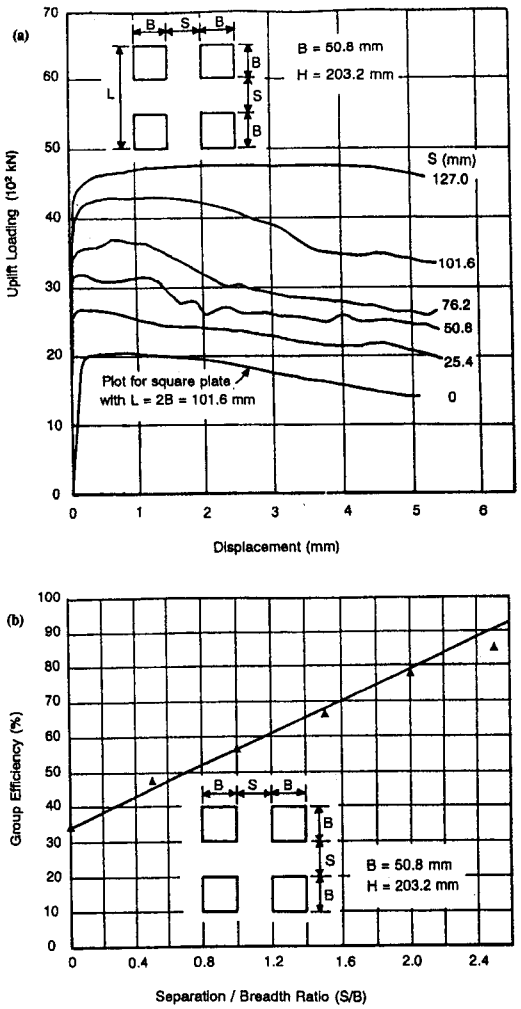

FIG. 3. Four Square Plate Configuration: (a) Load-Displacement Curves; (b) Group Efficiency versus Separation/Breadth Ratio

An isolated plate is defined as a plate that is not subject to interference from any other plates. The results are considered in detail in the following sections.

TWO-PLATE GROUPS

Fig. 2(a) shows the load/displacement relationships for a pair of square plates, at various separations (S), subjected to vertical uplift. The lowest curve with $S = 0$ is that for a single rectangular plate with a length/breadth ratio (L/B) = 2. In these tests, control was such that that differences between the total loads recorded on the proving ring and the sums of the load cell readings were less than 3% throughout, and the differences between the individual plate loads did not exceed 10%. The curves all display a rapid rise in resistance with displacement in the early stages, with a distinctive peak value at small displacement, followed by a progressive reduction as the displacement is increased. This pattern of behavior is attributable to the high density of the sand.

The effect of interaction of a pair of plates, at different separation ratios, is shown in the group efficiency plot of Fig. 2(b). The efficiency increases from about 59% for $S/B = 0$ to about 90% for $S/B = 2$, the maximum ratio used in the experiments. The initial part of the relationship is curved, but the later stages may be represented by a straight line. Overall, a straight line relationship as shown may be assumed to hold

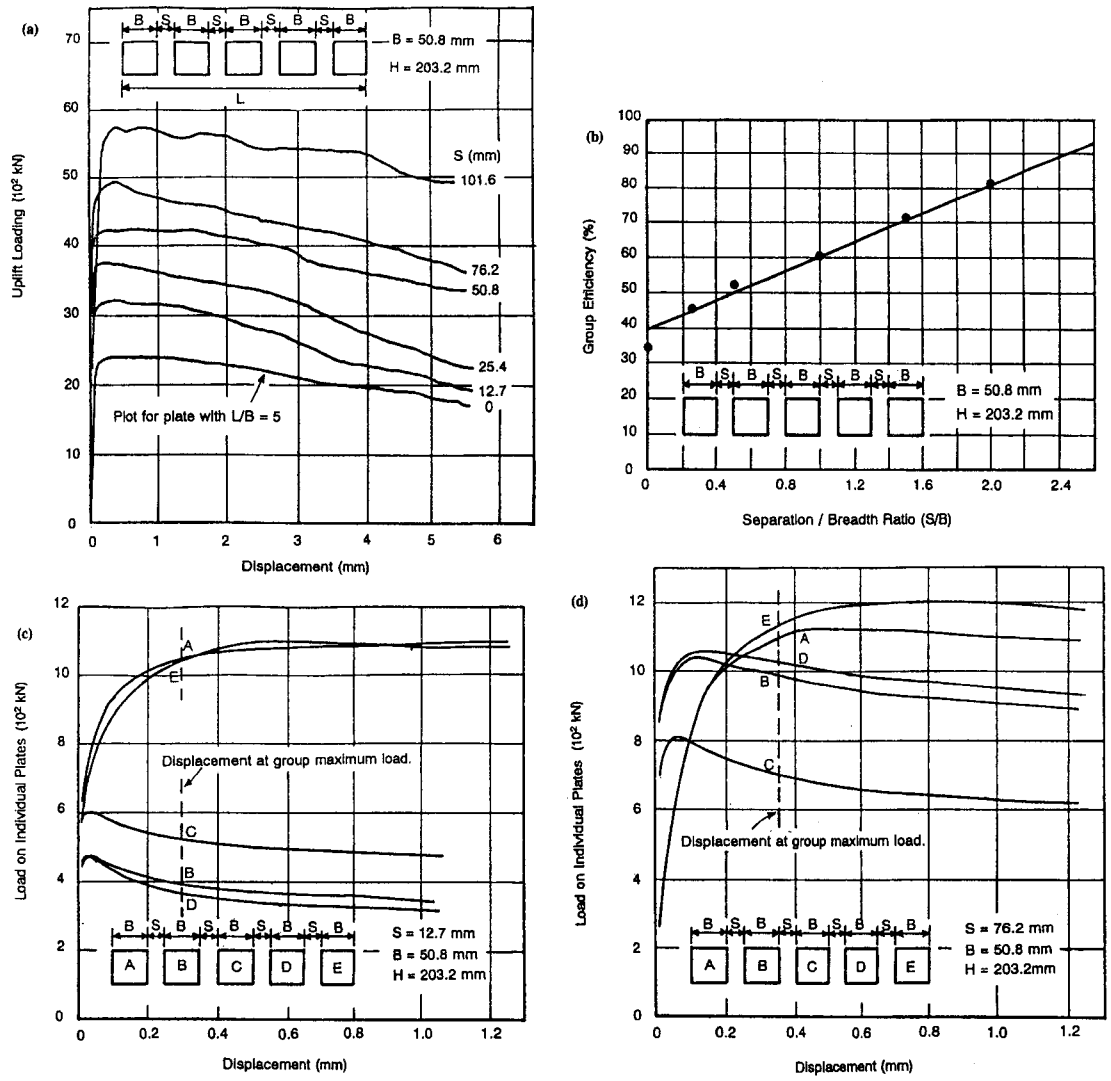

FIG. 4. Five Square Plate Row Configuration: (a) Load-Displacement Curves; (b) Group Efficiency versus Separation/Breadth Ratio; (c) Load-Displacement Curves for Individual Plates (S = 12.7 mm); (d) Load-Displacement Curves for Individual Plates (S = 76.2 mm)

with a reasonable accuracy, and this is considered at greater length later in the paper. At this stage, it may be remarked that an extrapolation of the curve to an efficiency value of 100% will render a value of S/B at which (and beyond which) there is no interference between the plates and, hence, there is independent action of each.

FOUR-PLATE GROUPS (SQUARE CONFIGURATION)

The load-displacement responses for four plates in square configurations are presented in Fig. 3(a). The lowest curve for $S = 0$ is that of a single square plate with $L = 2B = 101.6$ mm, i.e., twice the side length of the individual plates used in the other tests of the series. The differences between the recorded total loads and the sums of the load cell readings were always less than 4%. The loads carried by the individual plates did not differ by more than 20%. The behavior pattern is essentially similar to that described for the two-plate groups.

The group efficiency plotted against S/B ratio is shown in Fig. 3(b). The experimental points lie approximately on a straight line. With no separation (i.e., one plate of dimensions $2B \times 2B$) the efficiency is about 34%. This rises progressively toward a value of 100% as the separation is increased, to eventually bring about the independent action of the four plates comprising the system. For a specific S/B ratio, the efficiency of the group of four plates is markedly less than that of the group of two plates.

FIVE-PLATE GROUPS (ROW CONFIGURATION)

Fig. 4(a) illustrates the load-displacement relationships for the uplift of rows of five plates at different separations. The lowest curve, with $S = 0$, is that of a single rectangular plate with $L/B = 5$. In each test, the total proving ring load and the sum of the load cell readings for the individual plates corresponded within 4%. As for the two-plate and four-plate groups, the relationships are typified by a rapid rise to a distinctive peak resistance, followed by a progressive decline as displacements are increased.

The group efficiency relationship depicted in Fig. 4(b) once more demonstrates an initial "perturbation" followed by a straight-line mode of behavior. A straight-line approximation may be applied overall. The efficiency of the single plate is about 35%, and suitable extrapolation beyond the highest experimental S/B ratio of two can be expected to yield an eventual efficiency of 100%, i.e., no interference effects between the five plates.

Figs. 4(c–d) show the loads on the individual plates (A, B, C, D, and E) of the group as a function of displacement, for two of the spacings used. The dashed lines depict the displace-

ments at which the total loads (the sum for all five plates) were maxima. As the figures show, all plates do not reach their maximum resistance simultaneously. From these and other test results which are not shown, the three inner plates were found to reach their peak loads first, and then decline in their resistance as the end plates A and E moved to a maximum at substantially greater displacements. For all separations, the end plates reached individually higher ultimate loads than the inner plates. For all but the lowest separation ratio of 0.25 [Fig. 4(c)], the center plate of the group carried the lowest ultimate load.

COLLECTIVE BEHAVIOR PATTERNS

The preceding sections have presented the results of the sets of tests on different numbers and configurations of plates. This section analyzes the data in greater detail to portray consistent and logical behavior patterns, which should prove to be of benefit in predicting group anchor response to loading.

Load-Displacement Relationship

Points on the five curves of Fig. 2(a) have been replotted in Fig. 5 on the basis of a modified (normalized) value for the ordinate, expressed as

$$\frac{\text{load at given displacement}}{\text{peak load of the same curve}} \tag{2}$$

The points derived from each curve conform very closely to a single curve. Treating the results for the four-plate and five-plate groups in the same way also reduces them to the common curve of Fig. 5. This is shown in Table 1, which presents the average values of the normalized ordinates obtained from each set of experiments on a different number of plates.

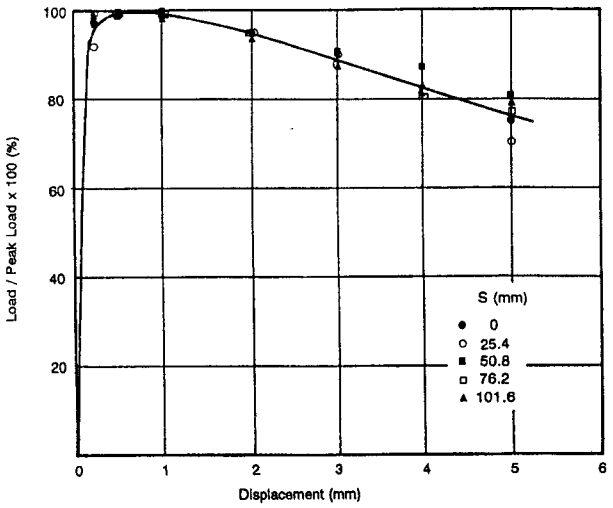

FIG. 5. Normalized Load-Displacement for Two Plates

TABLE 1. "Normalized" Curves of Group Load/Displacement; Values of Average Ratio of Load/Peak Load (×100)

Displacement (mm) (1)	Two-plate tests (2)	Four-plate tests (3)	Five-plate tests (4)	Overall average ratio (5)
0.25	97.1	98.1	98.8	98.0
0.50	99.2	98.3	99.8	99.1
1.00	99.1	97.9	98.2	98.4
2.00	94.6	92.7	94.3	93.9
3.00	89.3	86.7	87.4	87.8
4.00	82.4	82.0	80.4	81.7
5.00	76.4	78.4	74.5	76.4

For the conditions used in the experiments, all the load-displacement relationships may thus be derived, to a reasonable approximation, from a knowledge of the relationship for one test and a knowledge of the failure loading for each test.

Failure Loads

It was demonstrated earlier that the group efficiency versus separation ratio curves for each set of tests displayed similar characteristics [Figs. 2(b), 3(b), and 4(b)]. In Fig. 6(a) the experimental points of the three sets of results are replotted to a different coordinate sytem. The separation ratio (S/B) is replaced as the abscissa by L/B (i.e., ratio of the overall length of group/plate breadth), these being related by the expression

$$L/B = n + (n - 1)S/B \tag{3}$$

where n = number of plates per row.

The group efficiency is also replaced as the ordinate by the load factor, defined as

$$\text{load factor} = \frac{\text{peak load of group of } N \text{ plates}}{\text{peak load of a single isolated plate}} \tag{4}$$

This is linked to the group efficiency, as defined in (1) by

$$\text{load factor} = \text{group efficiency (\%)} \times N/100 \tag{5}$$

where N = total number of plates in the group.

The results of Fig. 6(a) for the two-plate and five-plate groups (row configurations) lie close to a straight line passing through the coordinate point (1,1), which is the point for a single isolated square plate of side B. For the two-anchor group, the load factor cannot exceed the value of 2 (two plates acting independently), which corresponds to L/B ratios ≥ 4.9. The latter from (3) corresponds to an S/B value of 2.9 and a group efficiency of 100%. For the row of five anchors, the limiting load factor of 5 is reached at $L/B = 16.6$, which also corresponds to an S/B value of 2.9. The intersection points of the limiting values of three-anchor and four-anchor groups equally give values of $S/B = 2.9$.

As shown in Appendix I, the equation of the line joining the experimental results is

$$\text{load factor} = 1 + \frac{\left(\frac{L}{B} - 1\right)}{\left(\frac{S_{crit}}{B} + 1\right)} \tag{6}$$

where S_{crit} = critical plate separation for maximum load factor and $S_{crit}/B = 2.9$ for the sand medium and overburden $H/B = 4$ used in the tests.

Eq. (6) is a relationship for rows of any number of anchors, and the form of the relationship is considered to be generally applicable, as will be demonstrated in the following. It is worth noting that (6) is independent of the number of plates.

There is, however, a deviation from this general relationship. The first points on the two-anchor and five-anchor curves lie below the general relationship and they may be connected by a straight line, which also passes through the coordinate position (1,1). The load factor for a rectangular plate is, thus, less than that for an anchor system with gaps, but of the same L/B ratio. For example, the load factor for a single plate of $L/B = 3$ is less than that for a two-plate anchor system with a separation ratio of $S/B = 1$ (i.e., $L/B = 3$, as for the single plate). On a similar basis, a single plate of $L/B = 8$ has a lower load factor than systems of three, four, five, six, and seven plates of $L/B = 8$, corresponding with the respective S/B values of 2.50, 1.33, 0.75, 0.40, and 0.17. There is a transition zone

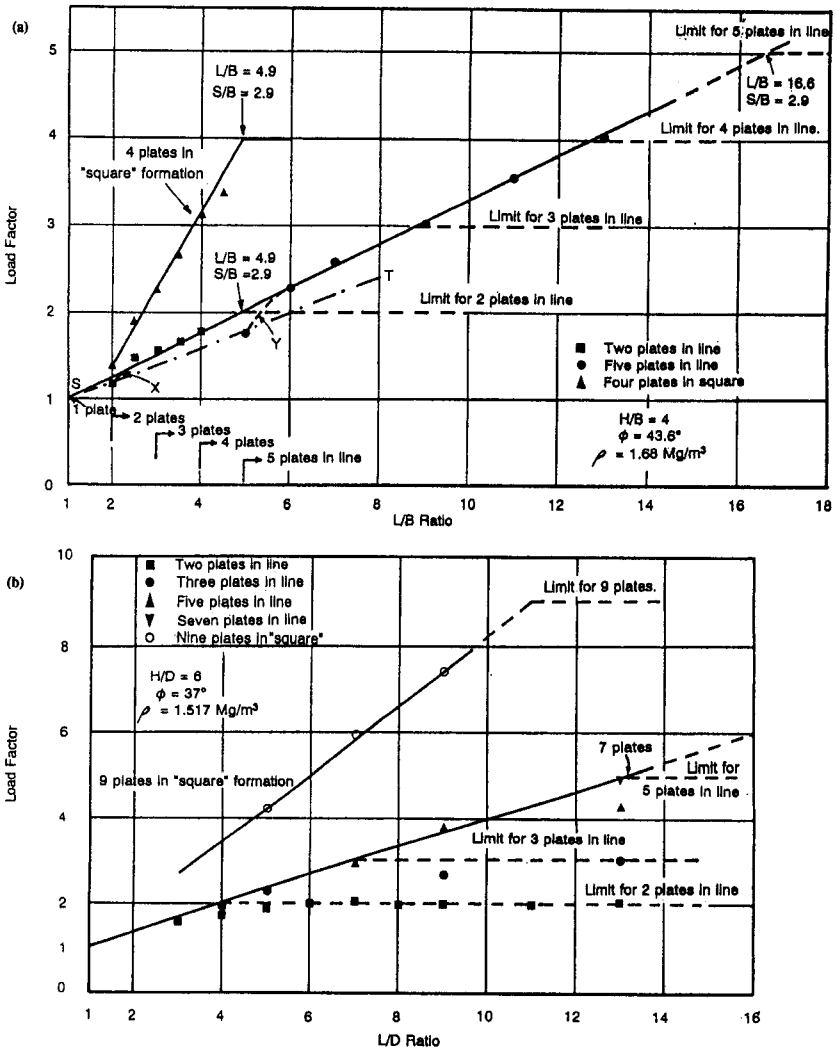

FIG. 6. Load Factor Plots for Plate Groups: (a) Load Factor versus *L/B* Ratio—Square Plates; (b) Load Factor versus *L/D* Ratio—Circular Plates [after Hanna (1972)]

from rectangular plate behavior to that of "developed" gap behavior, as shown by the curved zones marked X and Y.

Fig. 6(a) also aids in determining the L/B ratio for plates with gaps that are needed to produce the same load factor as a given rectangular plate, e.g., a rectangular plate of $L/B = 5$ has the same load factor (that is, carrying capacity) as a two-plate or three-plate system of $L/B = 3.9$ (S/B ratios of 1.9 and 0.45, respectively).

It is thus demonstrated that it is possible to achieve a greater load factor by cutting sections from a larger plate albeit necessary, in general, to ensure that the critical spacing is not exceeded. This situation arises because the resistance to uplift is a combination of the weight of sand within a truncated cone above the anchor plate and the shear resistance on the failure planes. For a single plate, the weight of sand is likely to be greater and the shear resistance less than for a row of plates with similar L/B. Between the plates forming the row, a complex mechanism of shear and dilation not experienced by the continuous plate more than compensates for any possible reduction in soil weight involved in uplift. This double dependency also explains the reason for the transition from rectangular plate behavior to developed gap behavior.

Based on an earlier paper (Murray and Geddes 1987), it is shown in Appendix II that the theoretical load factor for a stiff rectangular isolated anchor may be taken as

$$\text{load factor} = 1 + \frac{\left(\frac{L}{B} - 1\right)}{\left(\frac{H}{B}\tan\phi' + 1\right)} \tag{7}$$

Using this equation, the line S-T, passing through the coordinate point (1,1) may be constructed. This is seen to approximate closely to the line joining the experimental results for the rectangular isolated plates, although it should be noted that the analysis on which it is based does not reproduce the precise failure mechanisms of the experiments. Eq. (7) may be compared with (6) for the line joining interfering plates in a line formation.

The experimental results of the four-plate tests (square, rather than row configuration) also conform closely to a different straight-line relationship, as shown [Fig. 6(a)]. The curve turns to run parallel to the L/B axis at a limiting load factor of 4, and this produces a scaled change-point at $L/B = 4.9$ or, once more, $S/B = 2.9$ as for row configurations. Four anchors in a square formation produce much higher resistances than four anchors in a row formation over a very wide range of L/B values. On the other hand, two and three anchors in row formation can produce the same ultimate load (i.e., load factor) as four anchors in square formation, though at higher

L/B values. Also, with the square formation, the experimental point for $L/B = 2$ (no separation) lies close to that calculated theoretically in Appendix III.

The form of relationship for square plates in rows, shown in Fig. 6(a), appears to hold for other conditions. This is demonstrated by replotting the results for groups of circular plates in rows obtained by Hanna et al. (1972). Their results for two, three, five, and seven anchor plates do not show any clear relationship; but on replotting, as shown in Fig. 6(b), they are seen to conform to the same general pattern, with a critical S/D ratio (D is the diameter of the circular plates) of 2.0 for $H/D = 6$, $\phi' = 37°$, and $\gamma = 14.9$ kN/m^3. However, their results for nine circular plates in a square formation (3 × 3), while lying on a straight line, give rise to a critical S/D ratio of 4.0. This doubling of the critical S/D ratio does not appear to be reasonable and can only be resolved by further tests using circular plates.

Reverting to the tests on square plates in Fig. 6(a), the critical $S/B = 2.9$, below which it would be expected that adjacent failure cones would start to overlap and interact, corresponds to a failure cone angle to the vertical of 20°. As suggested by Vermeer and Sutjiadi (1985), among others, experimentation suggests this cone angle is close to the angle of dilation [i.e., in (6), $S_{crit} = 2H \tan \psi$, where ψ is the angle of dilation]. In the laboratory, anchor plate tests, stress levels, and soil stiffness will be small, and the dilation angle can consequently be expected to be large. An angle of dilation of around 20° would seem reasonable for the dense sand in the tests. In the tests on circular plates [Fig. 6(b)], the critical S/D ratio of 2 corresponds to an angle of inclination to the vertical of the failure surface of 10°. This again seems to be a reasonable value for the angle of dilation of this less-dense sand. In full-scale tests where the stress levels will be large and the mobilized shear strength and dilation will vary considerably along any failure surface, the effective angle of dilation and the angle of the cone to the vertical will be less than in the small-scale tests, which will consequently reduce the critical S/B or S/D ratio.

It is suggested from the foregoing that the kinds of relationships exhibited by Fig. 6(a) are applicable to sand mediums and H/B ratios other than those of the experiments. On this basis, equivalent diagrams may be calculated purely from a knowledge of ϕ using (7), and the critical S/B ratio using (6). It is tentatively suggested that the critical separation needed to produce independent anchor action is related to the dilation angle, which may prove useful in extending the predicted interaction effects to full-scale anchors if the dilation angle pertaining in situ can be assessed.

It is also interesting to examine the results of the two- and four- (i.e., 2 × 2) anchor configurations for square plates, as shown in Figs. 7 and 8. The former figure shows the relationship between the respective load factors at common L/B ratios. Over a substantial zone (i.e., for anchor plates with developed gap behavior) the experimental points may be approximated by a straight line which, when extrapolated, passes through the coordinate position (4,2), the theoretical and practical limiting value corresponding with $L/B = 4.9$ [see Fig. 6(a)], indicating a high degree of data consistency. The equation of the relationship is

$$LF_2 = 1.08 + 0.23LF_4 \quad \text{for the range } 1.9 \leq LF_4 \leq 4 \qquad (8)$$

in which LF_2 = load factor for two plates and LF_4 = load factor for four plates. Fig. 8 shows a plot of the load factor ratio against L/B in which

$$\text{load factor ratio} = \frac{\text{load factor for four plates (in square)}}{\text{load factor for two plates (in row)}} = \frac{LF_4}{LF_2} \qquad (9)$$

where both load factors are at the same L/B value. This produces a straight-line relationship over the range $2 \leq L/B \leq 4.9$ with the formula

$$\text{load factor ratio} = 0.564 + 0.293(L/B)$$

$$\text{For } (L/B) \geq 4.9 \quad \text{load factor ratio} = 2 \qquad (10)$$

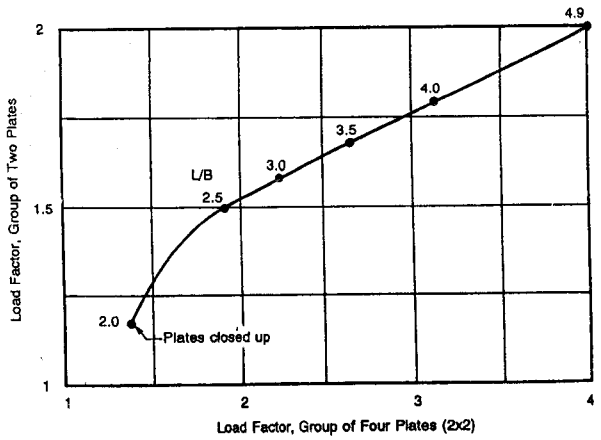

FIG. 7. Relationship between Load Factors

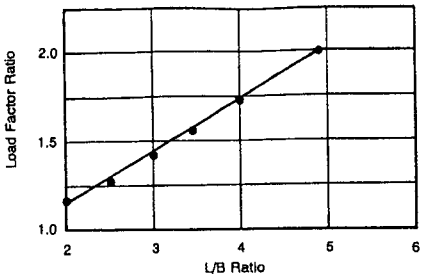

FIG. 8. Variation of Load Factor Ratio with L/B Ratio—Two and Four Plates

Load Distribution between Plates for Five-Plate Row Configuration

The manner in which the total load was distributed between the five individual anchors in a group was shown for two separations and at different displacements by Figs. 4(c) and 4(d). Fig. 9 shows the relationship between the separation ratio S/B and loads (individual anchor peak and at group peak) on the end anchors, central anchor, and intermediate anchors as a percentage of the peak load for an anchor plate acting separately. For the end and intermediate anchor plates, the plotted points are the mean of the two plate results.

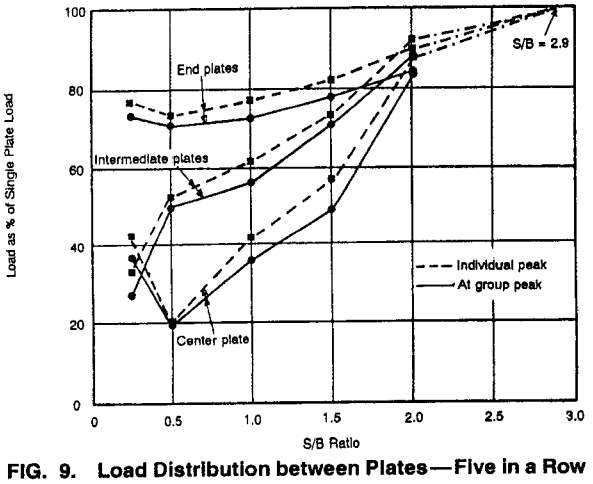

FIG. 9. Load Distribution between Plates—Five in a Row

The figure shows that, in general (at least for $S/B \geq 0.35$), the central anchor carried the least load and the outer anchors the greatest, in relation to both individual peak and group peak loads. The differences diminish as S/B increases. At an S/B ratio of 2, all anchors carry about the same load, which is in the order of 80%–90% of the maximum possible. It may be expected that for $2 \leq S/B \leq 2.9$, all anchors in the group carry a similar load, which converges on 100% of the maximum possible.

CONCLUSIONS

From the experiments carried out on square plate anchors in row and square configurations subjected to vertical uplift forces, several conclusions may be drawn. It is stressed that the results followed from the use of one depth of embedment ($H/B = 4$), in one dry sand medium placed at a single relative density, and with "static" loading applied in a displacement-controlled manner. Further investigations are needed to determine their full range of applicability. Thus, for the test conditions

- All the load-displacement curves for different numbers of anchors and configurations may be reduced to a single curve by normalizing them with respect to the peak load values. A single test result may, therefore, be used for prediction purposes when the associated peak load is known or can be estimated.
- The efficiency of a group of anchors (i.e., the peak load capacity as a proportion of that which could be carried by the total of the anchors acting as isolated anchors) increases from a relatively low value as the separation of the anchors is increased. At a critical separation ratio ($S/B = 2.9$ for the test conditions used), the maximum efficiency of 100% is reached and continues at that level with further increases in separation. This critical S/B value was valid for all configurations and numbers of plates. For each configuration, a different straight-line relationship may be used to link group efficiency and S/B value.
- The results of tests on rows of identical plates may be "unified" by plotting them in the form of load factor versus the ratio L/B (i.e., overall length of group/size of individual plates), where load factor (4) is defined as the ratio of the peak load capacity of the group to the peak load capacity of a single isolated plate anchor of the dimensions used in forming the group.

  This produces a straight-line relationship over most of the range of L/B and passes through the coordinate point (1,1). However, the value of the load factor cannot exceed the number of plates in the group. This occurs at L/B ratios corresponding to the critical value of S/B. The load factor values for isolated rectangular plates (i.e., $S/B = 0$) lie on a separate straight line of lesser gradient, but also pass through the coordinate point (1,1).

  The relationship for square configurations also takes a linear form with properties similar to the foregoing.

  As shown in the paper, it is possible to reproduce the curves from a limited amount of testing or a knowledge of the critical S/B ratio and equations defining the ultimate load capacity of isolated rectangular anchors (i.e., those without separation). It is tentatively suggested that if the effective angle of dilation is known, along with the mobilized angle of friction, the analyses can be used to predict the effect of interaction of shallow anchors in prototype anchor systems.
- The distribution for the maximum loads carried by the individual anchors in a linear group of five is a function of the S/B ratio. In general, the end anchors carry the greatest loads and the central anchor the least loads. All loads converge to an equal value (i.e., that of a single independent plate anchor) as the S/B value increases to its critical value.

APPENDIX I. DERIVATION OF EQUATION RELATING LOAD FACTOR AND SPACING FOR ROWS OF SQUARE PLATES

From Fig. 6(a), the general equation for the straight line joining the experimental results for plates in row configurations is given by

$$\text{load factor} = 1 + \left(\frac{L}{B} - 1\right) \times \text{slope of line} \tag{11}$$

When S equals S_{crit}, the separation for maximum load factor, the load factor equals n, where n is the number of plates in the row. At this spacing

$$\left(\frac{L}{B}\right)_{crit} = n + \frac{(n-1)}{B} S_{crit} \tag{12}$$

At this spacing

$$n = 1 + \left[\left(\frac{L}{B}\right)_{crit} - 1\right] \times \text{slope of line} \tag{13}$$

From (12)

$$n = 1 + \left[n + \frac{(n-1)}{B} S_{crit} - 1\right] \times \text{slope of line} \tag{14}$$

thus, the slope of the line in (11) for a row configuration is given by

$$\frac{1}{\frac{S_{crit}}{B} + 1} \tag{15}$$

which yields

$$\text{load factor} = 1 + \frac{\left(\frac{L}{B} - 1\right)}{\left(\frac{S_{crit}}{B} + 1\right)} \tag{16}$$

APPENDIX II. DERIVATION OF EQUATION FOR LOAD FACTOR FOR STIFF RECTANGULAR ISOLATED PLATE

The ultimate (peak) load capacity of a rectangular plate anchor subjected to vertical uplift may be represented by (Murray and Geddes 1987)

$$\frac{P_{rect}}{\gamma BLH} = 1 + \frac{H}{B}\tan\phi'\left(1 + \frac{B}{L} + \frac{\pi}{3}\frac{H}{L}\tan\phi'\right) \tag{17}$$

When $L = B$, i.e., for a square plate

$$\frac{P_{sq}}{\gamma B^2 H} = 1 + \frac{H}{B}\tan\phi'\left(2 + \frac{\pi}{3}\frac{H}{B}\tan\phi'\right) \tag{18}$$

As load factor = P_{rect}/P_{sq}, from (17) and (18)

load factor

$$= \frac{\frac{L}{B}\left(1 + \frac{H}{B}\tan\phi'\right) + \frac{H}{B}\tan\phi'\left(1 + \frac{\pi}{3}\frac{H}{B}\tan\phi'\right)}{\left(1 + \frac{H}{B}\tan\phi'\right) + \frac{H}{B}\tan\phi'\left(1 + \frac{\pi}{3}\frac{H}{B}\tan\phi'\right)} \tag{19}$$

For $\phi' = 43.6°$ and $H/B = 4$ (experimental values), when L/B equals 2, the load factor equals 1.20; when L/B equals 5, the load factor equals 1.81. These compare closely with the experimental values of Fig. 6(a). The equation for line S-T is obtained from (19) as follows:

$$\frac{P_{rect}}{P_{sq}} - 1 = (\text{load factor} - 1)$$

$$= \frac{\left(\frac{L}{B} - 1\right)\left(1 + \frac{H}{B}\tan\phi'\right)}{\left(1 + \frac{H}{B}\tan\phi'\right) + \frac{H}{B}\tan\phi'\left(1 + \frac{\pi}{3}\frac{H}{B}\tan\phi'\right)} \quad (20)$$

Therefore for a given ϕ' and H/B

$$(\text{load factor} - 1) = \text{constant} \times \left(\frac{L}{B} - 1\right) \quad (21)$$

This is the equation of a straight line through (1,1) with a slope of

$$\frac{\left(1 + \frac{H}{B}\tan\phi'\right)}{\left(1 + \frac{H}{B}\tan\phi'\right) + \frac{H}{B}\tan\phi'\left(1 + \frac{\pi}{3}\frac{H}{B}\tan\phi'\right)} \quad (22)$$

As an approximation, by writing $\pi/3 = 1$, the slope of line S-T is $1/[1 + (H/B)\tan\phi']$ which, for $H/B = 4$ and $\phi' = 43.6°$, the slope is $\tan^{-1}0.208$. Adopting the approximation, (20) may be written as

$$\text{load factor} = 1 + \frac{\left(\frac{L}{B} - 1\right)}{\left(\frac{H}{B}\tan\phi' + 1\right)} \quad (23)$$

APPENDIX III. DERIVATION OF EQUATION FOR LOAD FACTOR FOR SQUARE PLATE OF SIDE 2*B*

For a square configuration with a side equaling $2B$, from (18)

$$\text{load factor} = \frac{\gamma 4B^2H\left[1 + \frac{H}{2B}\tan\phi'\left(2 + \frac{\pi}{3}\frac{H}{2B}\tan\phi'\right)\right]}{\gamma B^2H\left[1 + \frac{H}{B}\tan\phi'\left(2 + \frac{\pi}{3}\frac{H}{B}\tan\phi'\right)\right]}$$

$$= 4 \times \frac{\left[1 + \frac{H}{2B}\tan\phi'\left(2 + \frac{\pi H}{6B}\tan\phi'\right)\right]}{\left[1 + \frac{H}{B}\tan\phi'\left(2 + \frac{\pi H}{3B}\tan\phi'\right)\right]} \quad (24)$$

For $H/B = 4$ and $\phi' = 43.6°$, the load factor = 1.45, a value close to the experimental one for a square configuration of four plates (i.e., $L/B = 2$).

APPENDIX IV. REFERENCES

Hanna, T. H., Sparks, R., and Yilmaz, M. (1972). "Anchor behavior in sand." *J. Soil Mech. and Found. Div.*, ASCE, 98(11), 1187–1207.

Hueckel, S. (1957). "Model tests on anchoring capacity of vertical and inclined plates." *Proc., 4th Int. Conf. on Soil Mech. and Found. Engrg.*, Butterworth Scientific Publications, London, 2, 203–206.

Larnach, W. J. (1972). "The pull-out resistance of inclined anchors installed singly and in groups in sand." *Ground Engrg.*, 5(4), 14–17.

Larnach, W. J. (1973). "Anchors 3—the behaviour of grouped inclined anchors in sand." *Ground Engrg.*, 6(6), 34–41.

Mayerhof, G. G. (1973a). "The uplift capacity of foundations under oblique loads." *Can. Geotech. J.*, Vol. 10, 64–70.

Meyerhof, G. G. (1973b). "Uplift resistance of inclined anchors and piles." *Proc., 8th Int. Conf. on Soil Mech. and Found. Engrg.*, USSR Nat. Spec. for Soil Mech. and Found. Engrg., Moscow, 2, 167–172.

Meyerhof, G. G., and Adams, J. L. (1968). "The ultimate uplift capacity of foundations." *Can. Geotech. J.*, 5(4), 225–244.

Murray, E. J. (1977). "The passive resistance of anchorages in sand," PhD thesis, Univ. of Wales, at Cardiff, U.K.

Murray, E. J., and Geddes, J. D. (1987). "Uplift of anchor plates in sand." *J. Geotech. Engrg.*, ASCE, 113(3), 202–215.

Neely, W. J. (1971). "The ultimate resistance of anchor plates in sand," PhD thesis, Queen's Univ. of Belfast, at Belfast, U.K.

Smith, J. E. (1962). "Deadman anchorages in sand." *U.S. Naval Civ. Engrg. Lab. Tech. Rep. No. R 199*, Port Hueneme, Calif.

Vermeer, P. A., and Sutjiadi, W. (1985)."The uplift resistance of shallow embedded anchors." *Proc., 11th Int. Conf. on Soil Mech. and Found. Engrg.*, A. A. Balkema, Rotterdam, The Netherlands, 3, 1635–1638.

APPENDIX V. NOTATION

The following symbols are used in this paper:

B = breadth of square anchor plate;
D = diameter of circular anchor plate;
H = depth from surface of sand to anchor plate level;
L = overall length of group of plates;
LF_2 = load factor for two plates;
LF_4 = load factor for four plates (square configuration);
$(L/B)_{crit}$ = value of (L/B) when $S = S_{crit}$;
P = ultimate (peak) load capacity of anchor system;
n = number of anchor plates in any row of anchor group;
N = total number of anchor plates in group;
P_{rect} = ultimate (peak) load capacity for rectangular plate anchor;
P_{sq} = ultimate (peak) load capacity for square plate anchor;
S = space between edges of successive (adjacent) plates;
S_{crit} = space between edges of successive plates when they just act as isolated plates;
c' = unit cohesion (effective stress);
γ = unit weight of sand;
ρ = density of sand (on Figs.);
ϕ' = angle of shearing resistance (effective stress); and
ψ = angle of dilation.